



Contents lists available at ScienceDirect

Catalysis Today

journal homepage: [www.elsevier.com/locate/cattod](http://www.elsevier.com/locate/cattod)

# High activity of Ga-containing nanosponge MTW zeolites in acylation of p-xylene

Jin Zhang, Ondřej Veselý\*, Mariya V. Shamzhy, Maksym Opanasenko, Jiří Čejka

Department of Physical and Macromolecular Chemistry, Faculty of Science, Charles University in Prague, Hlavova 2030, 12840 Prague 2, Czech Republic

## ARTICLE INFO

### Keywords:

MTW  
Gallosilicate  
Nanosponge  
Acylation of p-xylene

## ABSTRACT

Aluminosilicate and gallosilicate **MTW** zeolites were prepared in the bulk and nanosponge form by direct hydrothermal synthesis. Designed materials were tested in acylation of p-xylene with benzoyl chloride and compared with large pore zeolite **\*BEA** and medium pore zeolite **MFI**. Nanosponge **MTW** exhibited generally better performance than bulk **MTW** zeolites due to higher accessibility of the catalyst's active sites in nanosponge zeolite. Selective transformation of benzoyl chloride towards target 2,5-dimethylbenzophenone was achievable over nanosponge **MTW** zeolites. The gallosilicate nanosponge **MTW** exhibited significantly higher conversion (61%) of benzoyl chloride than its aluminosilicate counterpart (27%) with the same concentration of Brønsted acid sites (0.04 mmol/g). This result is clearly caused by the suitable strength of acid centres in Ga-MTW, which enables the sufficient activation of BzCl molecules as well as efficient desorption of formed polar products. Additionally, the gallosilicate **MTW** outperformed both conventional zeolites **\*BEA** and **MFI** used as reference materials.

## 1. Introduction

Zeolites are microporous aluminosilicates often applied in heterogeneous catalysis of petrochemical processes but also in fine chemical synthesis [1–10]. A unique property of the zeolites is the shape-selectivity; ability to admit or reject molecules to enter the micropores depending on their size and shape [3,7]. Moreover, the composition of zeolites may be altered to tune their acidic properties by replacing the aluminium, which gives the framework negative charge, by another tetrahedrally coordinated element (e.g. gallium, tin, titanium, iron). Each form is characteristic by different acidic properties and is suitable for catalysis of different reactions [11–15]. The shape-selectivity is one of the key features of zeolites applied in catalysis. However its drawback is the limited diffusion of reactant and product molecules through the confined space within the micropores. The diffusion can be facilitated by preparing zeolites with hierarchical system of pores. Besides the micropore system, hierarchical zeolites contain additional mesopores (2–50 nm wide) which enlarge their external surface and facilitate the mass transfer of the reactants/products to the active centres [16]. There are various methods for preparation of hierarchical materials. Direct synthesis, by the so called “soft-templating” method, which uses specially designed amphiphilic structure directing agents (SDAs), has attracted a lot of attention. The zeolite is prepared in a form called “nanosponge”, which consists of aggregated nanocrystals or nanosheets

with exceptional external surface [17,18].

Zeolites with acidity and the shape-selective properties are the most promising catalysts for the Friedel–Crafts acylations. Jacob et al. [19] studied the selectivity and activity of **\*BEA** in the acylation of p-xylene with benzoyl chloride (BzCl), it has been concluded that almost only monoacylated product 2,5-DMBP was formed with a BzCl conversion of 22.1% and a selectivity of 96.7%. Choudhary et al. [20] studied acylation of p-xylene with BzCl over  $\text{InCl}_3$  impregnated MCM-41, the yield of 2,5-DMBP was 74%. The selectivity and activity of FAU, **\*BEA** and **MFI** in the acylation of anisole with acetic anhydride were compared by Freese et al. [21] which indicated that **MFI** with smaller pores exhibited lower conversion of reactant compared to **\*BEA** and FAU. Laidlaw et al. [22] investigated the benzylation of substituted arenes with BzCl over Fe and Zn forms of H-ZSM-5, mordenite and zeolite Y, which demonstrated that Fe-exchanged zeolites can act as effective catalysts for heterogeneous benzylation. Recently, the catalytic performance of isomorphously substituted B-, Al-, Ga-, and Fe-containing extra-large-pore UTL zeolites in the acylation of p-xylene with BzCl was studied, it has been clarified that the activity of zeolites is closely related to the Brønsted acidity, (Ga)UTL zeolite with medium strength of Brønsted acid sites was characterized by the best activity and selectivity in the acylation of p-xylene with benzoyl chloride [23].

The goal of this work was to compare the performance of several zeolites and evaluate the effect of the framework topology, morphology

\* Corresponding author.

E-mail address: [veselyo5@natur.cuni.cz](mailto:veselyo5@natur.cuni.cz) (O. Veselý).

<https://doi.org/10.1016/j.cattod.2019.09.045>

Received 7 July 2019; Received in revised form 11 September 2019; Accepted 25 September 2019

0920-5861/© 2019 Elsevier B.V. All rights reserved.

and composition. Aluminosilicate and gallosilicate forms of zeolite **MTW** in bulk and hierarchical “nanosponge” form were tested in the acylation of toluene with benzoyl chloride. Also, conventional zeolites \***BEA** and **MFI** were tested for reference purposes.

## 2. Experimental section

### 2.1. Synthesis of zeolites

#### 2.1.1. Synthesis of SDAs

The synthesis of the nanosponge zeolites utilizes specially designed structure directing agents (“SDAs”), further denoted as „C22N6“. The preparation of C22N6 was performed by reaction of 1-bromodocosane with six times molar excess of N,N,N',N'-tetramethyl-1,6-diaminohexane in a mixture of toluene and acetonitrile (volume ratio 1:1; 25 ml per 1 g of 1-bromodocosane at 60 °C for 12 h. The solvents were evaporated and the product was washed with diethyl ether and dried at room temperature. Subsequently, the precursor is mixed with ten times molar excess of 1,4-bis(chloromethyl)benzene in a mixture of chloroform and acetonitrile volume ratio 2:1; 36 ml per 1 g of the precursor). The reaction was carried out at 65 °C for 24 h. Following, the solvents were evaporated, the product thoroughly washed with diethyl ether and acetone and then dried at room temperature. The product was mixed with half its molar amount of N,N,N',N'-tetramethyl-1,6-diaminohexane and dissolved in chloroform (6.3 ml per 1 g). The reaction was carried out at 85 °C for 24 h. Lastly, the chloroform was evaporated, the product was washed with diethyl ether and dried at room temperature. The purity of the final product was checked with <sup>1</sup>H NMR spectroscopy.

#### 2.1.2. Hydrothermal synthesis

The synthesis of aluminosilicate bulk **MTW** zeolite was carried out using tetraethylammonium hydroxide as SDA. Sodium aluminate was dissolved in distilled water and then TEA–OH was added. Colloidal silica (Ludox HS-40) was diluted to 30% with distilled water in a separate vessel. Both solutions were mixed together and homogenized by stirring. The final molar composition of the gel was 100 SiO<sub>2</sub> : 1 Al<sub>2</sub>O<sub>3</sub> : 1.46 Na<sub>2</sub>O : 25 SDA : 1330 H<sub>2</sub>O. The crystallization was carried out in a Teflon-lined steel autoclave at 160 °C for 6 days under static conditions. The product was recovered by filtration, washed with distilled water, dried at 65 °C and subsequently calcined in a flow of air at 550 °C for 6 h. Gallosilicate bulk **MTW** was prepared using the same procedure replacing the sodium aluminate with gallium nitrate. Additional sodium hydroxide was added to compensate for the sodium ions in sodium aluminate in order to keep the same molar composition of the mixture. The calcination of gallosilicate bulk **MTW** was carried out in a flow of air at 250 °C for 6 h followed by 450 °C for 2 h.

Aluminosilicate nanosponge **MTW** zeolite was prepared using the C22N6 as SDA. Sodium aluminate and sodium hydroxide were dissolved in water and the mixture was heated up to 60 °C. The SDA was added and when completely dissolved it was left to cool down to room temperature. The mixture was transferred to a polypropylene bottle, tetraethylorthosilicate was added and the whole bottle was shaken. The aging was carried out at 60 °C for 20 h. The final molar composition of the gel was 100 SiO<sub>2</sub> : 1 Al<sub>2</sub>O<sub>3</sub> : 13 Na<sub>2</sub>O : 3.333 SDA : 4500 H<sub>2</sub>O. The crystallization was carried out in a Teflon-lined steel autoclave at 150 °C for 6 days with rotation. The product was recovered by filtration, washed with distilled water and dried at 65 °C. The calcination was carried out under a flow of air at 580 °C for 8 h. Gallosilicate nanosponge **MTW** was prepared using the C22N6 as SDA following the same procedure. Sodium aluminate was replaced by gallium nitrate and additional sodium hydroxide was added to compensate for the sodium ions.

Commercial zeolites were purchased from Zeolyst International: \***BEA** (CP814E, Si/Al = 12.5) and **MFI** (CBV 3024E, Si/Al = 15).

### 2.2. Characterization

The structure and crystallinity of the zeolites were determined by X-ray powder diffraction using a Bruker AXS D8 Advance diffractometer equipped with a graphite monochromator and a position sensitive detector LYNXEYE XE-T using CuK $\alpha$  radiation in Bragg–Brentano geometry.

Argon adsorption/desorption isotherms were measured on a Micromeritics 3Flex volumetric Surface Area Analyser at 87 K to determine surface area, pore volume and pore size distribution. Before the sorption measurements, all samples were degassed in a Micromeritics Smart Vac Prep instrument under vacuum at 250 °C (heating rate 1 °C/min) for 8 h. The specific surface area was evaluated by BET method using adsorption data in the range of a relative pressure from  $p/p^0 = 0.05$  to  $p/p^0 = 0.25$ . The DFT method was applied to determine the volume of micropores (V<sub>mic</sub>). The adsorbed amount at relative pressure  $p/p^0 = 0.98$  reflects the total adsorption capacity (V<sub>tot</sub>). The pore size distributions were calculated using the BJH model from the desorption branch of the isotherms.

TEM imaging was performed using JEOL NEOARM 200 F with a Schottky-type field emission gun at accelerating voltage of 200 kV. Microscope was equipped with TVIPS XF416 CMOS camera. The alignment was performed using standard gold nanoparticles film method. Due to low beam-stability of the sample the dose of electrons was kept below current density of 2 pA/cm<sup>2</sup>.

The concentration and type of acid sites were determined by adsorption of pyridine as a probe molecule and observed by FTIR spectroscopy Nicolet 6700 AEM equipped with DTGS detector, using the self-supported wafer technique. Prior to adsorption of the probe molecule, self-supported wafers of zeolite samples were activated in-situ by overnight evacuation at temperature 450 °C. Pyridine adsorption proceeded at 150 °C for 20 min at partial pressure 3 Torr, followed by 20 min evacuation at 150 °C or 450 °C. The concentrations of Brønsted and Lewis acid sites in aluminosilicate samples were calculated from integral intensities of individual bands characteristic of pyridine on Brønsted acid sites at 1545 cm<sup>-1</sup> and band of pyridine on Lewis acid site at 1455 cm<sup>-1</sup> and molar absorption coefficients of  $\epsilon(B) = 1.67 \pm 0.1 \text{ cm} \cdot \mu\text{mol}^{-1}$  and  $\epsilon(L) = 2.22 \pm 0.1 \text{ cm} \cdot \mu\text{mol}^{-1}$ , respectively. The spectra were recorded with a resolution of 4 cm<sup>-1</sup> by collection 128 scans for single spectrum.

The purity of prepared organic SDAs was verified by measuring <sup>1</sup>H NMR spectra on a Varian Mercury 300 MHz spectrometer. D4 methanol was used as the solvent.

### 2.3. Acylation of *p*-xylene

The catalytic tests were performed in the liquid phase under atmospheric pressure at 130 °C in a multi-experiment workstation StarFish. Prior to the experiment, 50 mg of the catalyst was activated at 450 °C for 90 min with a rate of 10 °C/min. Then 5 ml of *p*-xylene, 0.25 g of *n*-dodecane and the catalyst (for a blank experiment the catalyst was not used) were placed in a three-necked vessel equipped with a condenser and a thermometer and heated to the reaction temperature. When the desired temperature was achieved, 5 mmol of benzoyl chloride were added into the vessel to start the reaction. Then, samples of the reaction mixture were taken in 0 min, 10 min, 30 min, 1 h, 2 h, 3 h, 4 h, and 5 h. When the sample was taken it was centrifuged to remove the catalyst and remaining solution was analysed by gas chromatography. Gas chromatograph Agilent 7890B GC equipped with HP-5 column (length 30 m, diameter 0.320 mm, and film thickness 0.25  $\mu\text{m}$ ) and flame ionization detector was used for the analysis.

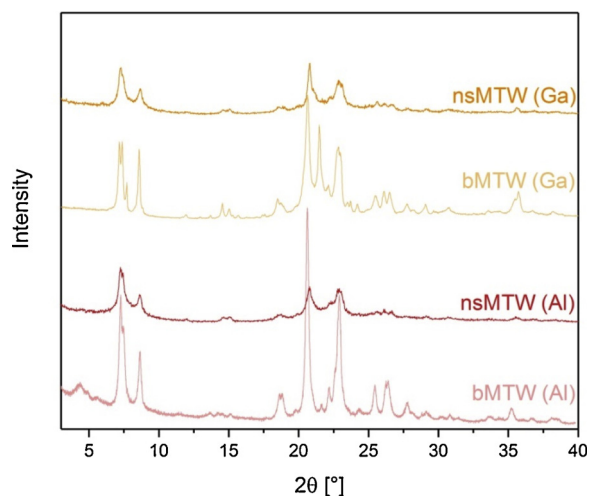


Fig. 1. X-Ray powder diffraction patterns of the MTW samples.

### 3. Results and discussion

#### 3.1. Characterization of bulk and nanosponge MTW

MTW zeolite samples were prepared in the form of aluminosilicate (labelled with “(Al)” suffix) and gallosilicate (labelled with “(Ga)” suffix), both in the bulk (denoted as “bMTW”) and nanosponge form (denoted as “nsMTW”). The diffraction patterns of the samples in Fig. 1 matches well with the simulated powder patterns in the database. Broadening of the diffraction lines of both nanosponge samples is a result of their thin-crystal-like morphology.

Textural properties of the bulk and nanosponge MTW samples were investigated by the adsorption of argon (Fig. 2). The isotherms of bulk samples are nearly flat above the relative pressure 0.05, signifying their microporous nature. On the other hand the isotherms of both nanosponge samples keep increasing, which indicates presence of mesopores as can be seen from the pore size distribution. Relatively thin hysteresis loop of the nanosponge samples suggests majority of the mesopores is directly accessible from the external surface. Textural properties listed in the Table 1 show clear difference between the two morphologies, especially in the means of their external surface areas and pore volumes.

Transmission electron microscopy was used to investigate the morphology of the MTW samples (Fig. 3). Both bulk samples are composed of well defined crystallites 50–100 nm in size. On the other

Table 1

Textural properties of the MTW and commercial MFI, \*BEA samples based on the argon adsorption and their chemical composition.

Sample	Si/T	S <sub>BET</sub> [m <sup>2</sup> /g]	S <sub>ext</sub> [m <sup>2</sup> /g]	V <sub>tot</sub> [cm <sup>3</sup> /g]	V <sub>mic</sub> [cm <sup>3</sup> /g]
bMTW (Al)	52	292	57	0.220	0.130
nsMTW (Al)	49	516	405	0.981	0.125
bMTW (Ga)	n.d.	223	67	0.170	0.110
nsMTW (Ga)	88	396	161	0.674	0.100
MFI	16.3	376	112	0.241	0.118
*BEA	12.6	641	212	0.700	0.195

n.d. – not determined.

hand, the nanosponge samples are formed of aggregated small crystalline domains (10–30 nm in size).

The FTIR measurement of the MTW samples after adsorption of pyridine was used to investigate the concentration of Brønsted and Lewis acid sites (Fig. 3). Each spectrum contains a peak at 1545 cm<sup>-1</sup> which corresponds to a pyridine adsorbed on Brønsted sites. Another peaks which lie at 1455 cm<sup>-1</sup> and 1445 cm<sup>-1</sup> belong to a pyridine adsorbed on Lewis acid sites of strong and weak Lewis acid sites, respectively. As shown in Fig. 4, the aluminosilicate bulk MTW is predominantly Brønsted acidic with 0.11 mmol/g compared to 0.03 mmol/g of Lewis acid sites. On the other hand the nanosponge form contains slightly more Lewis sites (0.06 mmol/g) than Brønsted sites (0.05 mmol/g). Concentrations of acid sites in both gallosilicate MTW zeolites are comparable and noticeably lower than respective acid site concentrations of their aluminosilicate counterparts.

We compared the concentration of acid sites retained pyridine after desorption at 150 °C and 450 °C to assess the fraction of “strong” acid centres in isomorphously substituted MTW zeolites of different morphologies (Fig. 6). The percentage of “strong” acid centres in bMTW (Al) and nsMTW(Al) totalled 42–43%, while bMTW(Ga) and nsMTW (Ga) possessed only 27 and 13% of “strong” acid sites, respectively. Thus, a relative concentration of “strong” acid sites increases in the following sequence of MTW zeolites: nsMTW(Ga) < bMTW(Ga) < nsMTW(Al) = bMTW(Al).

#### 3.2. Catalysis over MTW zeolite samples

Catalytic activity of bulk and nanosponge zeolites containing acid sites of different nature (Al and Ga centres) was compared in the Friedel-Crafts acylation reaction (Scheme 1). This reaction was chosen to distinguish the catalytic properties of designed MTW samples because it is known to be sensitive to the accessibility and strength of active sites. To study the effect of active sites accessibility, we can

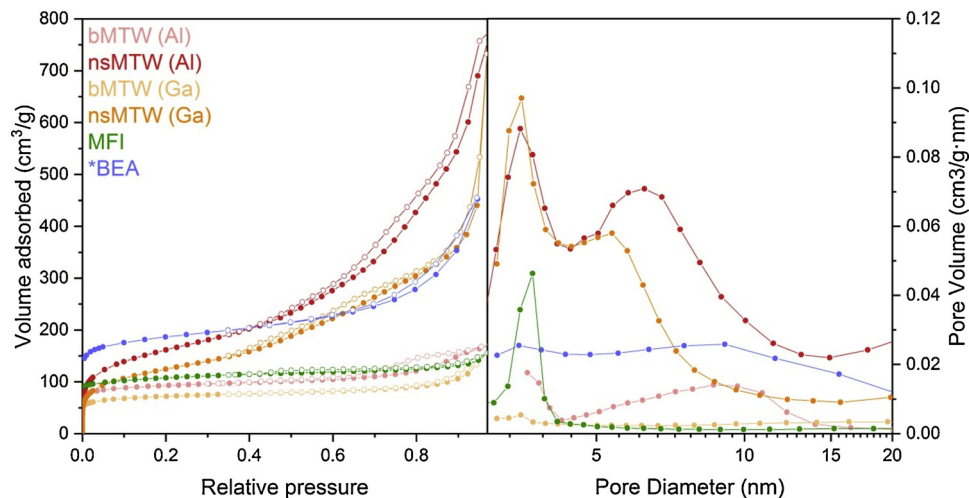


Fig. 2. Argon adsorption isotherms and pore size distributions of the MTW and commercial MFI, \*BEA samples.

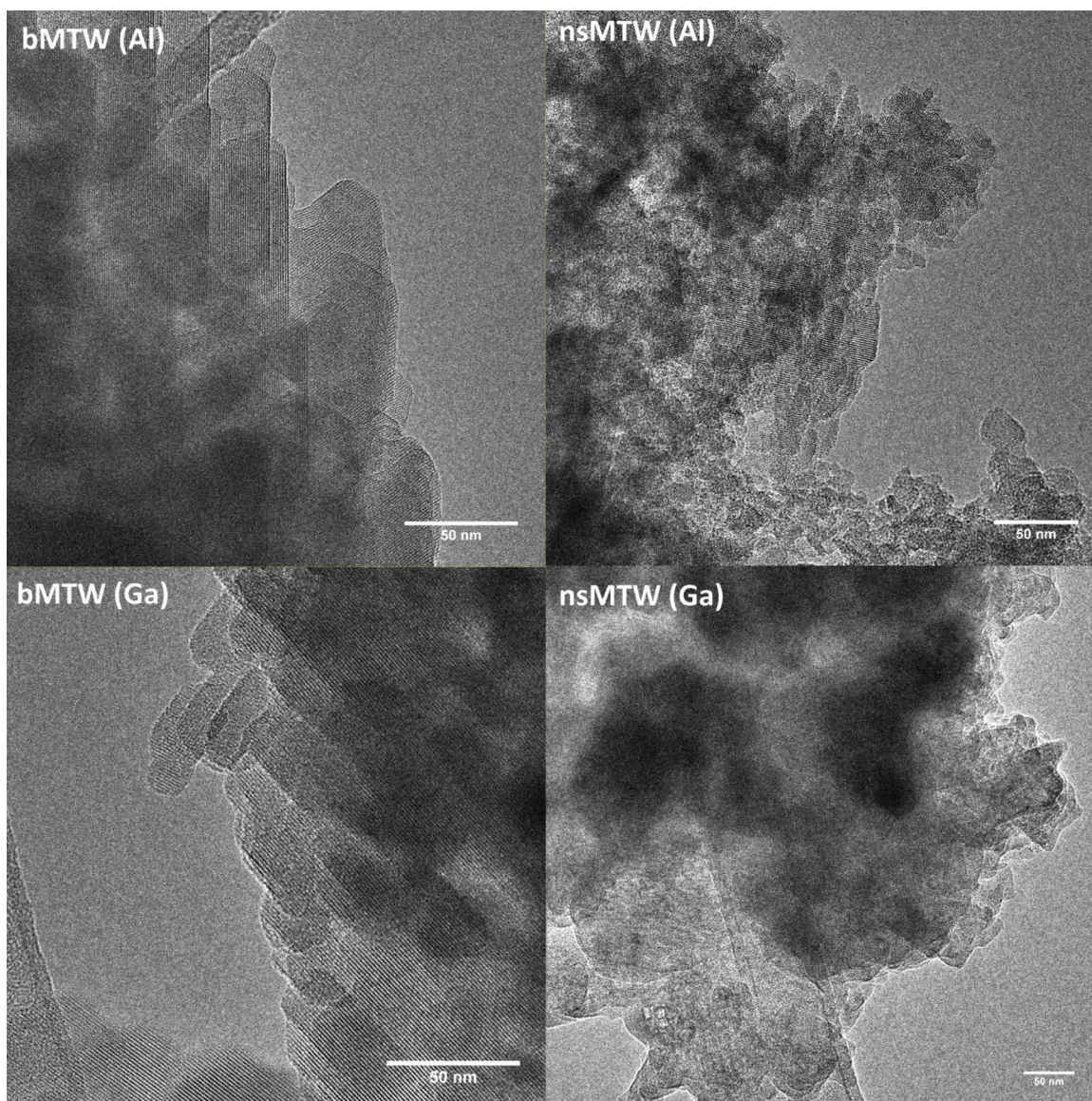


Fig. 3. Transmission electron microscopy images of the MTW samples.

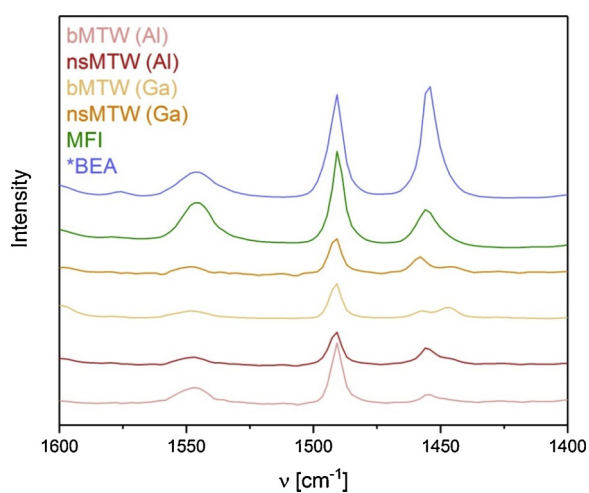
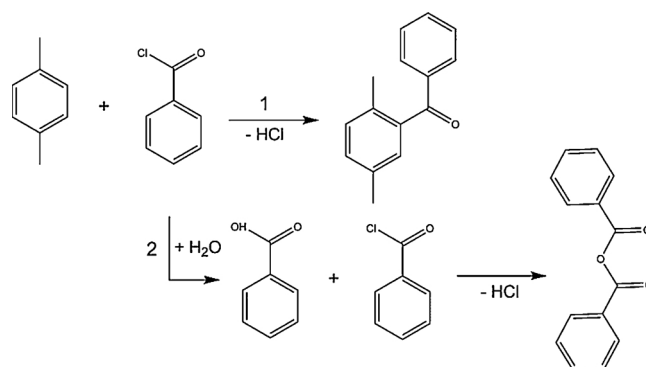


Fig. 4. FTIR spectra of MTW and commercial MFI, \*BEA samples after the adsorption of pyridine.



Scheme 1. Acylation of p-xylene with benzoyl chloride (1) accompanied by the hydrolysis of BzCl (2).

compare the catalytic behaviour of bulk and nanosponge samples containing same type of three-valent element. To investigate the influence of acid site strength, materials with the same morphology (either bulk or nanosponge) but different type of catalytic centres (Al vs. Ga) have to be compared.

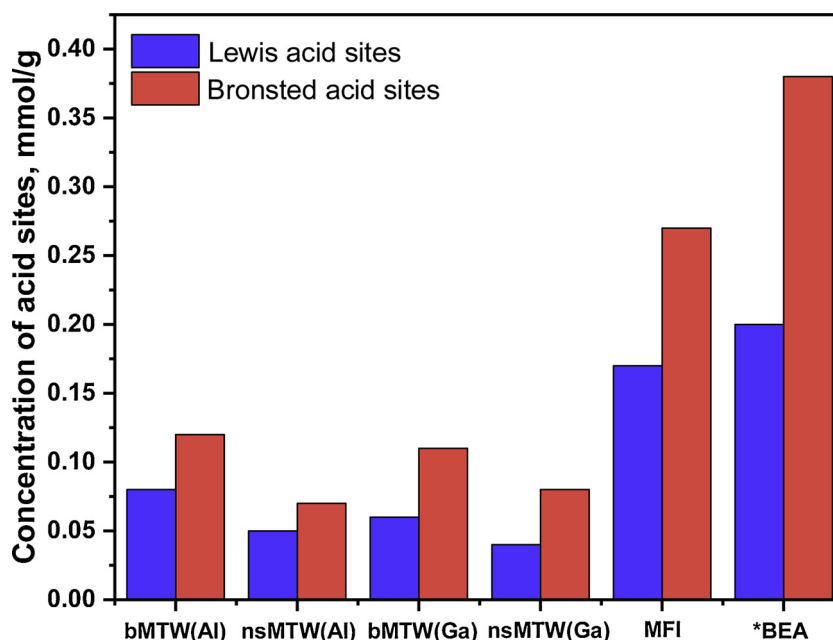


Fig. 5. Acidic properties of MTW and commercial MFI, \*BEA samples.

2,5-Dimethylbenzophenone (2,5-DMBP) is the main product in the acylation of *p*-xylene with benzoyl chloride (BzCl), while main side reactions are hydrolysis of benzoyl chloride to form benzoic acid (BA) or benzoic anhydride (BAC) especially important if the catalyst contains only weak Lewis acid sites [9,24,25]. MFI and \*BEA zeolites with three-dimensional pore systems (in contrast to one-dimensional in MTW) were used as reference materials, whereas blank experiment was performed to understand the extent of non-catalysed hydrolysis processes (towards BA and BAC).

In general, the conversion of BzCl over MFI and bMTW(Al) were comparable and did not significantly exceed the consumption of BzCl in blank experiment carried out without catalyst. At the same time, the target product 2, 5-DMBP was not detected in all three experiments indicating that benzoyl chloride was hydrolysed to form BA and BAC. In contrast, nsMTW(Al) and especially nsMTW(Ga) exhibited significantly

higher conversions outperforming even the \*BEA catalyst possessing three-dimensional porosity with larger pore entrances and higher concentration of acid sites (Figs. 5 and 7).

To analyze the effect of topology and morphology on the catalytic behaviour of MTW zeolites, we have compared the catalytic properties of gallosilicate and aluminosilicate bulk MTW with the corresponding nanosponge zeolites. The conversion of BzCl over both nanosponge MTW zeolites (61% for nsMTW(Ga) and 27% for nsMTW(Al)) was much higher than that of the bulk analogues (25% for bMTW(Ga) and only 6% for bMTW(Al)) (Fig. 7a). This result is clearly caused by improved accessibility of the catalyst's active sites in nanosponge zeolites as a result of well-developed mesoporosity.

Comparison of nanosponge MTW zeolites with similar concentration of both Brønsted (0.07 – 0.08 mmol/g) and Lewis acid sites (0.04–0.05 mmol/g), but different in the acid site nature (Al or Ga) and thus

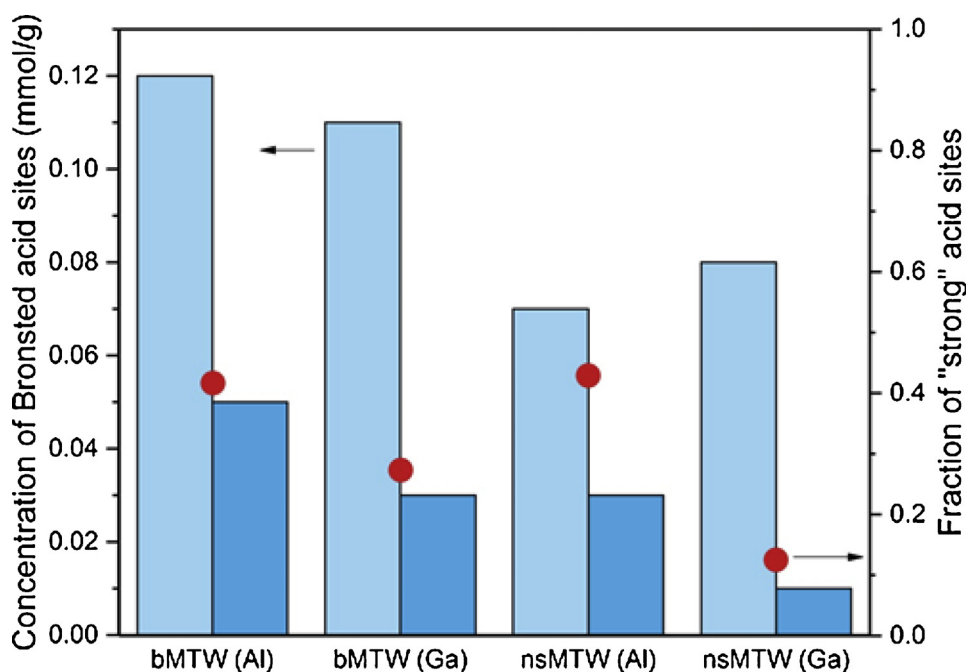


Fig. 6. Concentration of Brønsted acid sites of the MTW samples after desorption at 150 °C (light blue) and 450 °C (dark blue). The ratio between the concentration of acid sites determined at 450 °C and 150 °C is shown as (red dot).

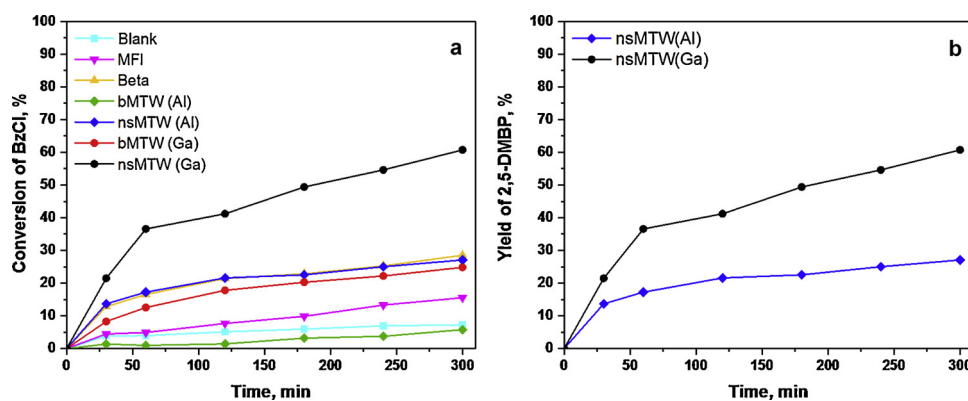


Fig. 7. Conversions of benzoyl chloride (a) and yield of 2, 5-DMBP (b) over MTW samples.

their strength. Yield of the 2,5-DMBP over the nanosponge samples correlates well with the conversion of BzCl and no side-products were detected (Fig. 7b). It means both gallosilicate and aluminosilicate nanosponge MTW zeolites selectively catalyse acylation of p-xylene with BzCl. However, the conversion of BzCl significantly increases with decrease in the strength of active sites (conversion is 61% for nsMTW(Ga) vs. 27% for nsMTW(Al)) with no effect on the selectivity towards 2,5-DMBP. This result is presumably caused by the decreasing rate of the target 2,5-DMBP desorption from the active sites with the increase in the strength of Brønsted acid sites. As the consequence of longer residence time, Al sites are not able to activate BzCl molecules as efficiently as Ga centres. Our results are consistent with previous studies, which indicated that the optimum strength of acid sites is required to achieve the highest conversion of reactants in acylation reaction [23]. Ergo, nsMTW(Ga) is assumed to demonstrate the optimal activity in the acylation of p-xylene within benzoyl chloride in comparison with nsMTW(Al) because of the suitable strength of acid centres in former sample, which enables the sufficient activation of BzCl molecules as well as efficient desorption of formed 2,5-DMBP.

#### 4. Conclusions

Aluminosilicate and gallosilicate MTW zeolites were prepared in the bulk and nanosponge form by the direct hydrothermal synthesis. P-xylene acylation with benzoyl chloride was investigated using the MTW samples, along with large-pore zeolite \*BEA and medium-pore zeolite MFI for comparison. The reaction over MFI and bMTW(Al) did not lead to the formation of target 2,5-DMBP product. On the other hand, bMTW (Ga), nsMTW(Ga) and nsMTW(Al) successfully catalysed the transformation of BzCl to the desired product. Due to the higher accessibility of the catalyst's active sites in nanosponge zeolite, both aluminosilicate and gallosilicate nanosponge MTW zeolites exhibited better catalytic performance than the bulk MTW zeolites. At the same time, nsMTW (Ga) with optimum strength of Brønsted acid sites exhibited highest yield of 2,5-DMBP (61%) among catalysts studied due to the balanced strength of acid centres, which enables the sufficient activation of BzCl molecules as well as efficient desorption of formed 2,5-DMBP products. This study shows that gallosilicate nanosponge zeolites can be the promising catalysts in acylation reactions.

#### Acknowledgement

OV acknowledges the Czech Science Foundation for the ExPro project (19-27551X).

#### References

[1] M. Bejblova, D. Prochazkova, J. Cejka, Acylation reactions over zeolites and mesoporous

catalysts, *ChemSusChem* 2 (2009) 486–499.  
 [2] C.P. Bezouhanova, Synthesis of aromatic ketones in the presence of zeolite catalysts, *Appl. Catal. A* 229 (2002) 127–133.  
 [3] J. Cejka, H. Van Bekkum, A. Corma, F. Schueth, Introduction to Zeolite Molecular Sieves, (2007).  
 [4] J.M. Escola, D.P. Serrano, R. Sanz, R.A. Garcia, A. Peral, I. Moreno, M. Linares, Synthesis of hierarchical Beta zeolite with uniform mesopores: effect on its catalytic activity for veratrole acylation, *Catal. Today* 304 (2018) 89–96.  
 [5] M. Kantam, K. Ranganath, M. Sateesh, K. Kumar, B. Choudary, Friedel–Crafts acylation of aromatics and heteroaromatics by beta zeolite, *J. Mol. Catal. A Chem.* 225 (2005) 15–20.  
 [6] M. Koehle, Z.Q. Zhang, K.A. Goulas, S. Caratzoulas, D.G. Vlachos, R.F. Lobo, Acylation of methylfuran with Brønsted and Lewis acid zeolites, *Appl. Catal. A* 564 (2018) 90–101.  
 [7] D. Kubicka, I. Kubickova, J. Cejka, Application of molecular sieves in transformations of biomass and biomass-derived feedstocks, *Catal. Rev. Sci. Eng.* 55 (2013) 1–78.  
 [8] X. Rao, H. Ishitani, W.J. Yoo, S. Kobayashi, Zirconium- $\beta$  zeolite-catalyzed continuous-flow Friedel–Crafts acylation reaction, *Asian J. Org. Chem.* 8 (2019) 316–319.  
 [9] G. Sartori, R. Maggi, Use of solid catalysts in Friedel–Crafts acylation reactions, *Chem. Rev.* 106 (2006) 1077–1104.  
 [10] H. Van Bekkum, A.J. Hoefnagel, M.A. Van Koten, E.A. Gunnewegh, A.H.G. Vogt, H.W. Kouwenhoven, Zeolite catalyzed aromatic acylation and related reaches, *Stud. Surf. Sci. Catal.* (1994) 379–390.  
 [11] V.R. Choudhary, S.K. Jana, N.S. Patil, S.K. Bhargava, Friedel–Crafts type benzylation and benzylation of aromatic compounds over H $\beta$  zeolite modified by oxides or chlorides of gallium and indium, *Microporous Mesoporous Mater.* 57 (2003) 21–35.  
 [12] K.M. Konyshcheva, P.S. Yaremov, Z.V. Chernenko, S. Filonenko, O.V. Shvets, Effect of nature of heteroelement (Ba, Ga, Al) on adsorption and acid characteristics of hierarchical porous zeolites of MOR, BEA, and MTW structural types, *Theor. Exper. Chem.* 53 (2018) 410–416.  
 [13] X. Liu, L. Zhang, H. Xu, J.G. Jiang, M.M. Peng, P. Wu, Pore size-tunable titanosilicates post-synthesized from germanosilicate by structural reorganization and H $_2$ TiF $_6$ -assisted isomorphous substitution, *Appl. Catal. A* 550 (2018) 11–19.  
 [14] M. Shamzhy, M. Opanasenko, P. Concepcion, A. Martinez, New trends in tailoring active sites in zeolite-based catalysts, *Chem. Soc. Rev.* 48 (2019) 1095–1149.  
 [15] O.V. Shvets, K.M. Konyshcheva, M.M. Kurmach, Morphology and catalytic properties of hierarchical zeolites with MOR, BEA, MFI, and MTW topology, *Theor. Exp. Chem.* 54 (2018) 138–145.  
 [16] J. Pech, P. Pizarro, D.P. Serrano, J. Cejka, From 3D to 2D zeolite catalytic materials, *Chem. Soc. Rev.* 47 (2018) 8263–8306.  
 [17] W. Kim, J.-C. Kim, J. Kim, Y. Seo, R. Ryoo, External surface catalytic sites of surfactant-tailored nanomorphous zeolites for benzene isopropylation to cumene, *ACS Catal.* 3 (2013) 192–195.  
 [18] C. Jo, K. Cho, J. Kim, R. Ryoo, MFI zeolite nanosponges possessing uniform mesopores generated by bulk crystal seeding in the hierarchical surfactant-directed synthesis, *Chem. Commun.* 50 (2014) 4175–4177.  
 [19] B. Jacob, S. Sugunan, A.P. Singh, Selective benzylation of o-xylene to 3,4-dimethylbenzophenone using various zeolite catalysts, *J. Mol. Catal. A Chem.* 139 (1999) 43–53.  
 [20] V.R. Choudhary, S.K. Jana, N.S. Patil, Acylation of aromatic compounds using moisture insensitive InCl $_3$  impregnated mesoporous Si-MCM-41 catalyst, *Tetrahedron Lett.* 43 (2002) 1105–1107.  
 [21] U. Freese, F. Heinrich, F. Roessner, Acylation of aromatic compounds on H-Beta zeolites, *Catal. Today* 49 (1999) 237–244.  
 [22] P. Laidlaw, D. Bethell, S.M. Brown, G.J. Hutchings, Benzylation of substituted arenes using Zn- and Fe-exchanged zeolites as catalysts, *J. Mol. Catal. A Chem.* 174 (2001) 187–191.  
 [23] M.V. Shamzhy, O.V. Shvets, M.V. Opanasenko, L. Kurfiřtová, D. Kubicka, J. Cejka, Extra-large-pore zeolites with UTL topology: control of the catalytic activity by variation in the nature of the active sites, *ChemCatChem* 5 (2013) 1891–1898.  
 [24] B. Chiche, A. Finiels, C. Gauthier, P. Geneste, J. Graille, D. Pioch, Friedel–Crafts acylation of toluene and p-xylene with carboxylic acids catalyzed by zeolites, *J. Org. Chem.* 51 (1986) 2128–2130.  
 [25] M.V. Shamzhy, O.V. Shvets, M.V. Opanasenko, P.S. Yaremov, L.G. Sarkisyan, P. Chlubná, A. Zukal, V.R. Marthala, M. Hartmann, J. Cejka, Synthesis of isomorphously substituted extra-large pore UTL zeolites, *J. Mater. Chem.* 22 (2012) 15793–15803.